Growth and bonding structure of hard hydrogenated amorphous carbon thin films deposited from an electron cyclotron resonance plasma

O. Durand-Drouhin, M. Lejeune, and M. Benlahsen

Citation: Journal of Applied Physics **91**, 867 (2002); doi: 10.1063/1.1423786
View online: http://dx.doi.org/10.1063/1.1423786
View Table of Contents: http://scitation.aip.org/content/aip/journal/jap/91/2?ver=pdfcov
Published by the AIP Publishing

Growth and bonding structure of hard hydrogenated amorphous carbon thin films deposited from an electron cyclotron resonance plasma

O. Durand-Drouhin, M. Lejeune, and M. Benlahsen[a)]
Laboratoire de Physique de la Matière Condensée, Faculté des Sciences d'Amiens, 33 rue Saint Leu, 80039 Amiens Cedex 2, France

(Received 8 February 2001; accepted for publication 9 October 2001)

Analysis of hard hydrogenated amorphous carbon films (a-C:H) deposited from an electron cyclotron resonance radio frequency discharge of methane–argon (5%) mixture at low pressure is reported. The properties of films were determined in their as deposited state using elastic recoil detection analysis, infrared absorption, Raman spectroscopy, transmission spectroscopy, photothermal deflexion spectroscopy, and residual stress measurements. The microstructural changes (i.e., hydrogen content and C-sp^3/C-sp^2 ratio) have been explained qualitatively in terms of a balance between implantation and relaxation processes. A good correlation is observed between the variation of Raman features and the optical gap as a function of the self-bias substrate. The residual stress versus bias plot shows behavior similar to that already obtained for tetrahedral amorphous carbon films and the optimum energy, which corresponds to films of maximum C–C sp^3, is similar to those obtained in the literature. © *2002 American Institute of Physics.* [DOI: 10.1063/1.1423786]

I. INTRODUCTION

The understanding of hard hydrogenated amorphous carbon films (a-C:H) [so-called diamond-like carbon (DLC)] growth and microstructure remains problematic and of great interest.[1–4] DLC films are generally amorphous and contain a significant fraction of sp^3-C bonding and their microstructure can be defined as a metastable and highly dense form of amorphous carbon.[5–8] This metastable structure likely originates from the interaction of energetic ions with the surface of the growing film,[5–9] which affects the hydrogen content and bonding, and thus the hybridization type of carbon atoms and the properties of DLC films.[10–13]

Different mechanisms for the formation of the sp^3 rich phase have been proposed,[6–8] among these, the subimplantation model proposed by Davis and Robertson to describe the tetrahedral amorphous carbon films (ta-C) formation.[7,8] This model suggests that the impinging particles are supposed to be sufficiently energetic to penetrate the surface and randomly displace carbon atoms from their equilibrium positions in the films through a series of primary and recoil collisions producing both volumetric distortion and intrinsic stress development.[7–9] The probability of penetration increases with energy, and then at higher energies the probability of relaxation increases, giving rise to an optimum energy for densification sp^3 bonding.[10–16] For the tetrahedral hydrogenated amorphous carbon films (ta-C:H), the deposition processes are considered as a combination of the subimplantation processes describing ta-C and those additional, possibly ion-assisted processes needed to describe the reactions of radicals such as striking, abstraction, and the elimination of hydrogen.[10,12]

The aim of this article is to describe the deposition mechanism and the microstructure changes in hydrogenated DLC films prepared by plasma enhanced chemical vapor deposition of methane–argon (5%) mixture at low pressure, in a dual electron cyclotron resonance radio frequency (ECR-rf) glow discharge. In the ECR plasma, the electrons, having relatively high energy, generate ionic species in a significant amount increasing the more diamond-like form of a-C:H. The microwave excitation provides a denser plasma and the rf bias allows good control of the mean energy of the ions impinging on the surface of the substrate.[17,18] The interaction of plasma species with the growing film influences mainly the material microstructure (i.e., H content and C-sp^3/C-sp^2 ratio). Most properties of as-deposited a-C:H films such as optical gap and stress are interpreted on the basis of the subimplantation process and discussed in terms of a balance between implantation and relaxation processes.

II. EXPERIMENTAL DETAILS

Hard a-C:H films about 0.4 μm thick, measured with a Dektak III profilometer, were deposited from an ECR-rf glow discharge plasma (excited at 2.45 GHz power) of methane–argon (5%) gas mixture. A constant value of 150 W is used to excite the gas introduced at a flow rate of 13 sccm. Silicon and quartz substrates were chemically cleaned in an ultrasonic bath prior to deposition and placed on a rf-driven electrode (13.56 MHz) kept at room temperature. The plasma pressure was about 0.35 Pa and the induced negative bias voltage V_b, which is related to the ion energy at low pressure, ranged from -30 to -600 V corresponding to a rf power of 4 and 80 W, respectively. The bias voltage effect is to control the ion energy during film growth. The ion energy depends on two factors: the acceleration potential across the grid sheath and the energy loss by collision in the sheath.

a)Author to whom correspondence should be addressed; electronic mail: mohamed.benlahsen@sc.u-picardie.fr

This source is operated at low pressure (2.6 mTorr) to minimize ion collisions, and uses a magnetic field to product plasma ionization and to confine the plasma. The deposition apparatus is described in detail elsewhere.[17,18]

The film vibrational properties are investigated by Fourier transform infrared (FTIR) absorption spectroscopy using a NICOLET Fourier transform spectrometer at room temperature over a large wave number range, from 400 to 4000 cm^{-1}, with a resolution of 4 cm^{-1} and averaging over 500 scans in samples deposited on c-Si substrate. The total H content is determined by elastic recoil detection analysis (ERDA). Raman spectra were performed at room temperature with a Dilor Z24 triple monochromator using the 514.5 nm line of an argon ion laser. The laser power was limited to 50 mW in order to prevent any material heating and damage. A combination of photothermal deflexion spectroscopy (PDS) measurements and the optical transmission ones in the 300–3000 nm range were used in order to determine the refractive index n at 2 μm and the optical gap using a Varian Cary 5 spectrometer.

The stress σ in the films is determined from the curvature measurements of the silicon wafer, before and after film deposition, by using a Dektak III profilometer and Stoney's equation

$$\sigma = \frac{E_s}{6(1-\nu_s)} \frac{h_s^2}{h_f} \left(\frac{1}{R_2} - \frac{1}{R_1} \right),$$

where $E_s/(1-\nu_s)$ is the substrate biaxial modulus, equal to 180.5 GPa for (100)-oriented Si substrates; h_s and h_f are the substrate and the film thickness, respectively; and R_1 and R_2 are the radii of curvature of Si substrates before and after deposition of films, respectively.

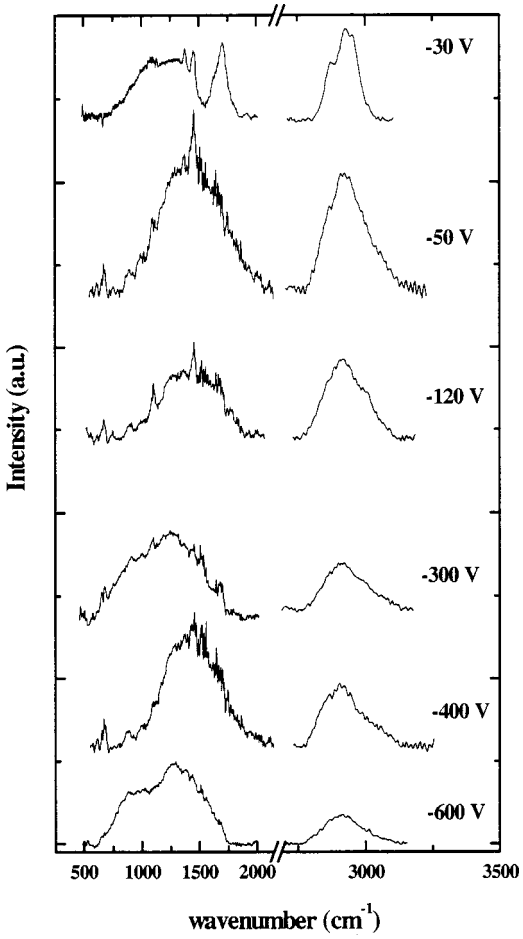

FIG. 1. Typical IR spectra obtained in the C–H stretching band region for films deposited at different bias voltage in their as-deposited state.

III. RESULTS AND DISCUSSION

The composition of the ECR-rf plasma of methane and the structural properties of the resulting films have been reported elsewhere.[17,18] It was reported that in the ECR plasma the electrons, having relatively high energy, generate ionic species in a significant amount. In addition, the dominant dissociation channels for methane produces ions like CH_x^+ and possesses high hydrogen content. The growing surface of a-C:H films is also highly hydrogenated. The role of hydrogen is primarily to saturate π bonds, converting sp^2 sites into sp^3 sites. For the present study, ERDA measurements show that the H content is relatively high and decreases from 44 to 31 at. % as the negative bias increases in absolute magnitude from -30 to -600 V. The possible rise in the substrate temperature at high bias voltage is relatively insufficient to explain the desorption of hydrogen from the film during deposition.[17–20] As previously reported, the bias voltage appears to increase the kinetic energy of the incident ions, which can play a role not only in the surface processes, but also in the composition and the microstructure of the a-C:H film.[10,12,13,17] The highly energetic ions can break C–H bonds and create new C–C bonds, leading to a decrease of the H amount incorporated in the films as a function of bias voltage.[1,13,17–21]

A. IR measurements

The effect of the bias voltage on the C–H bonding is illustrated in Fig. 1 by the modifications of the IR spectra for samples deposited under various bias voltages in their as-deposited state. These bands are decomposed into Gaussian components corresponding to the different possible vibrational modes of the C–H bond.[19,22] The analysis of these results leads to the following observations:

(i) All series exhibit similar proportion of H bonded to sp^3-C sites determined from the integrated intensity of the subbands below 3000 cm^{-1} in CH_2 as well as CH_3 configurations. The decrease in the total bonded H content in the films could be result of the breaking of the C–H bonds caused by an increase in the substrate bombardment by ion species arising from the increase in the bias voltage, as previously reported.[13,17,23–25] This result is consistent with the ERDA measurements noted above.

(ii) The band centered around 3450 cm^{-1}, can be related to the two broad bands centered around 1700 and 1060 cm^{-1}, also observed only for series deposited at -30 V and suggest a high contamination by oxygen and water (C═O, C–O bond stretching modes). This result indicates that this series presents a strong open porosity, that is a large fraction of void networks in these films.

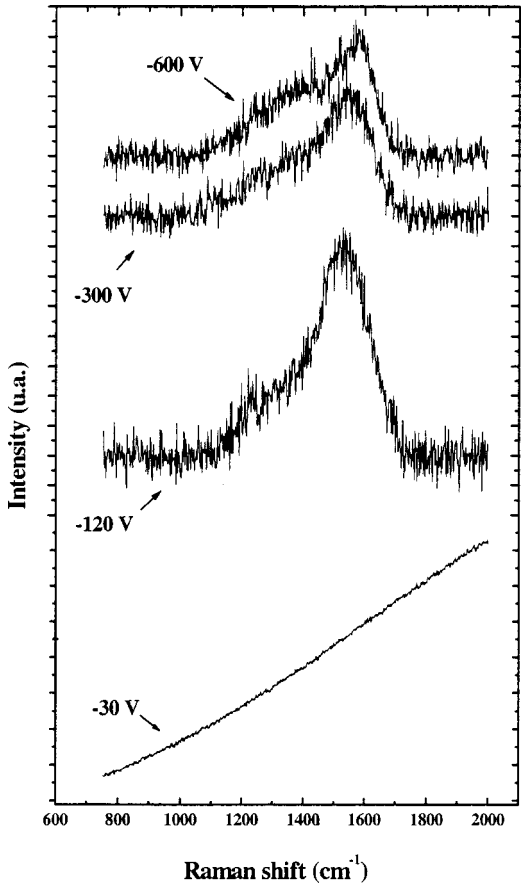

FIG. 2. Typical Raman spectra at room temperature for samples grown under different substrate bias. The excitation wavelength is 514 nm. The irradiated spot of the sample was about 3 mm^2 wide with a total incident laser power of 50 mW.

(iii) The proportion of the H bonded to sp^2-C site in olefinic chains and aromatic ring configurations (band around 3000 and 3050 cm^{-1}), depends on the bias voltage range.[12] For low bias voltage values, from -30 to about -120 V, essentially olefinic configurations are found, while being confirmed by the 850–950 cm^{-1} bands associated with wagging modes of C═CH_2 groups. The increase observed in the intensity of the peak centered around 1580 cm^{-1}, which is associated with the C═C double bond as a function of the bias voltage, suggesting a reorganization of the carbon atoms for a more aromatic configurations.[24]

B. Raman spectra

Figure 2 shows the Raman spectra of the films deposited at -30, -120, -300, and -600 V, respectively. The spectra of all samples (except those deposited at -30 V) are very similar, and exhibit the two usual features seen in sp^2-bonded carbons:[26] the *G* peak around 1550 cm^{-1} and the disorder (*D*) mode around 1360 cm^{-1}. The *G* mode arises from the Raman-active zone-center mode of graphite, while the *D* mode is the disorder-activated mode of sp^2-bonded crystallites.

For series deposited at -30 V, the Raman spectrum is totally masked by the photoluminescence (PL) band. As previously reported, the PL is due to the radiative recombination of electron hole pairs within sp^2 bonded clusters in an sp^3 bonded amorphous matrix.[4] The confinements of photoexcited electron–hole pairs in the graphitic clusters might control the PL. The PL intensity tends to increase with increasing H concentration due primarily to the saturation of nonradiative recombination sites.[4] At higher bias voltage, -120 V, the photoluminescence disappears and the Raman bands appear. The *G* peak is broad, consistent with its large stress, disorder, and high sp^3 content.[27,28,30] At high bias voltage, the *G* peak evolution traduces a transition to sp^2 bonded C and is consistent with the decrease in hydrogen content reported both by ERDA and IR measurements. The *D* peak is, however, relatively broad.

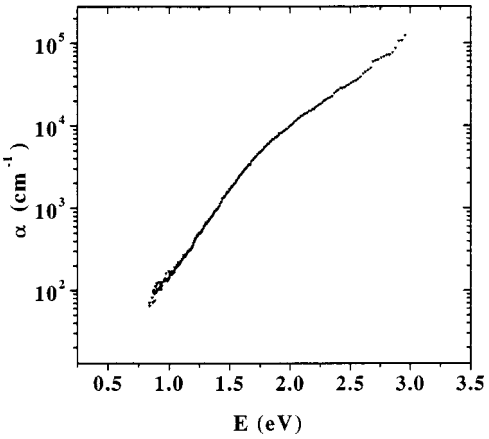

FIG. 3. Raman characteristics as a function of the substrate bias: (a) positions of the maximum value for each line (*G* and *D*); (b) FWHM of the *D* and *G* (ΔG and ΔD) lines in the different Raman spectra.

Peak positions for these films were determined by fitting the experimental Raman spectra by Gaussian profile with background correction. All the fitting parameters such as the full width at half maximum (FWHM) of the *G* and *D* lines; their positions and their integrated intensity ratio I_D/I_G were variable. Figure 3 shows the *G* line and *D* line positions (a) and the *G* and *D* widths (b) as a function of the bias voltage. The correlation between the *G* and *D* peaks evolution and ion energy is similar to that found for ta-C and ta-C:H.[27–30] The *G* peak moves up from 1519 to 1576 cm^{-1} with increasing bias voltage, while the *D* peak moves down from 1342 to 1394 cm^{-1}, as shown on Fig. 3(a). In addition, the width of the *G* peak (ΔG) passes through a maximum value of about 193 cm^{-1} for -120 V and remains large due to the disordering effect of ion bombardment [Fig. 3(b)]. This maximum corresponds to films of C–C-sp^3 content.[27] The width of the *D* peak (ΔD) is always greater than ΔG and decreases from 246 to 226 cm^{-1} for -120 V and then increases for higher bias, so there remains some disorder likely, due to the ion bombardment effect. The integrated intensity ratio I_D/I_G increases from the very low value of 0.35 to 2.12. The range of the I_D/I_G ratios is characteristic of highly tetrahedral amorphous carbon films.[10,12,14] According to Tuinstra and Koenig the integrated intensity ratio I_D/I_G varies inversely with crystalline size L_a in the microcrystalline region.[29] Using the Ferrari and Robertson formula,[30] in which the disorder is

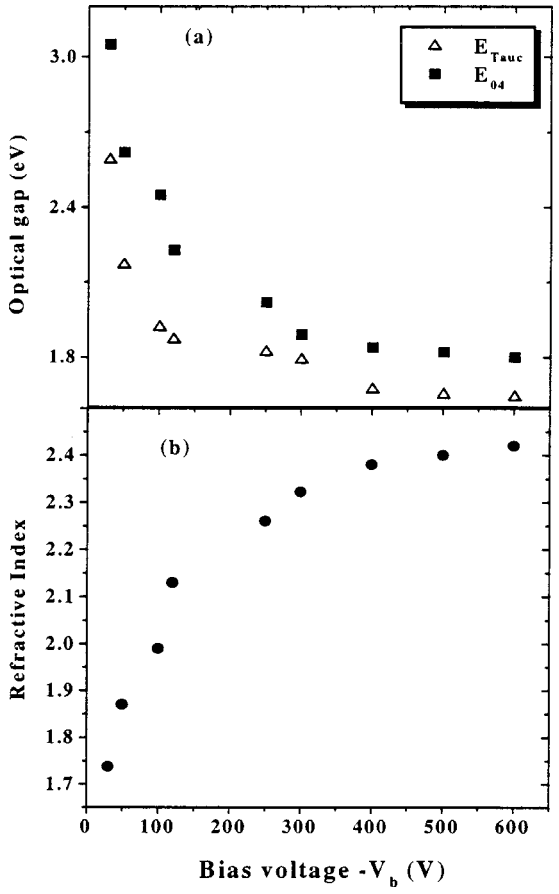

FIG. 4. Optical absorption spectra of hydrogenated DLC films deposited at bias voltage about −120 V.

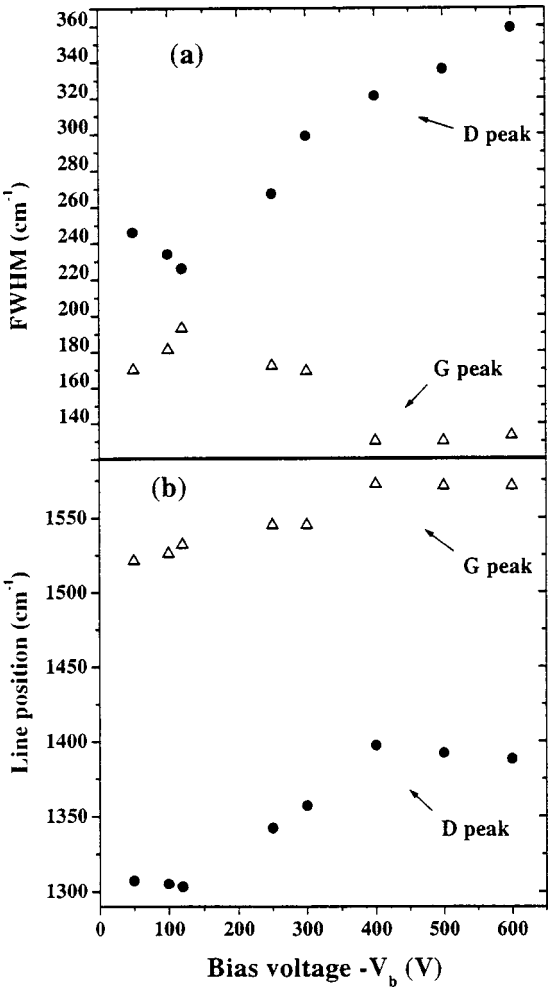

FIG. 5. Variation of E_{Tauc} and E_{04} (a) and the refractive index n (b) as a function of the bias voltage obtained for the as-deposition films.

included, L_a never exceeds about 20 Å when the bias voltage varies from −120 to −600 V.

C. Optical properties

The optical-absorption coefficient α for films deposited at −120 V on quartz substrates as the function of energy in the absorption edge region is illustrated in Fig. 4. The energy is obtained by a combination of optical transmission and PDS measurements. The optical gap E_{Tauc} of semiconductors is conventionally defined by the Tauc relationship[31] $\alpha E = B(E - E_{\mathrm{Tauc}})$.[2] However, the E_{04} gap, defined as the energy at which the optical-absorption coefficient reaches $10^4\ \mathrm{cm}^{-1}$, is generally regarded as a more reliable value of the gap for a situation of very broad absorption edges, such as here.

Figures 5(a) and 5(b) plot the variation of the optical gaps, both E_{04} and E_{Tauc} (Tauc gap), and the refractive index n (determined at 2 μm) against the bias voltage. The E_{04} gap is larger than E_{Tauc} and they, as usual, decrease rapidly as the bias increases from −30 to −300 V and then remains almost constant for higher bias.[23–25] This behavior can be caused by the decrease of H content and a recombination of defects or by reduction of the disordering in the film due to the increase in the amount of sp^2-C sites. It is also suggested by IR measurements, which show the increase in the proportions of the sp^2-(C–H) as the bias varies from −30 to −300 V. For higher bias, the sp^2-(C–H) proportion seems to vary only very slightly. In the mean time, the refractive index n increases in the same range of bias and then reaches a saturation value for bias higher than −300 V, as shown in Fig. 5(b). The increase in n suggests an increase in the film density as the H content decreases due to the impact of high energy ions.

It is now believed that the optical gap in amorphous carbon films is determined by the gap between the π states and the π^* states on sp^2, and is controlled by the sp^2 bonding, which tends to pair up, to form larger clusters in a mainly sp^3 matrix.[4] The dissociation of the species after impact at the surface can affect this trend by the degree of disorder associated with the energetic bombardment, which could oppose ring clustering and distort the local planar configuration of C-sp^2 atoms influencing mainly the optical response of the film.[4,32] The creation of defects and ion-inducing disordering of the carbon network occurs only in the range of the impinging ions during the deposition process.

The dependence of the optical gap on the sp^2 size and the disorder effect may be expected from Raman spectra.[27,30] We plot in Figs. 6(a) and 6(b) the I_D/I_G ratio and the G linewidth (ΔG) against the E_{Tauc}. The correlation between the fitting parameters (i.e., I_D/I_G ratio and ΔG) behaviors

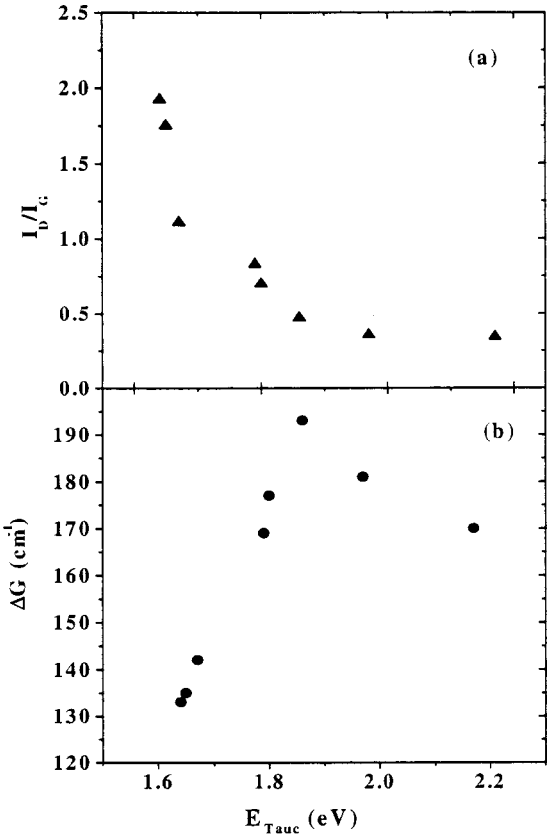

FIG. 6. Variation of the intensity ratio I_D/I_G (a), and the FWHM of the G line (ΔG) (b) as a function of E_{Tauc}.

and the E_{Tauc} is similar to that found for a-C:H.[27,30] As noted above the I_D/I_G ratio evolution is characteristic of a transition to more graphitic a-C:H films and suggests that it is still a very highly disordered form of C-sp^2. In a-C:H films, the C-sp^2 sites can exist as rings as well as chains and the main effect of H is to modify the C–C network. At low bias voltage (low I_D/I_G ratio), most of the sp^3 sites are bonded to H and the films consist of isolated sp^2-bonded clusters and thus, the band gap is high. The gradual change in the band gap seems to be related to the width of the π band, which depends on the cluster size such that the optical gap depends inversely on L_a deduced from the Raman measurements.[4,32] Nevertheless the optical responses of the film not only work for the assumption of cluster size but also with the degree of disorder associated with the ion bombardment.[4,30,32–34] Indeed, at high bias voltage (high I_D/I_G ratio), the H content is low and C-sp^2 dominates. The decline observed in Fig. 6(a) of the I_D/I_G ratio with increasing E_{Tauc} traduces a decrease of the average sp^2 cluster size L_a using the Ferrari and Robertson formula.[30] In this case, the optical response results form a dynamic equilibrium of the disordering, due to the ion bombardment, in carbon network (distortions of the π bonding) and the rearrangement of the covalent network (relaxation process). So, the band gap depends on both cluster size and the local distortions of the π bonding.[32–34]

For completeness, in Fig. 6(b) we also presented the variation of ΔG versus E_{Tauc}. It is seen that ΔG increases with decreasing E_{Tauc}. Until it reaches a maximum at around 1.87 eV for bias voltage about -120 V, and then decreases gradually for the lower optical gap. This value is of the same order as those obtained in a-C:H and can be correlated with maximal density and hardness (maximum C–C sp^3 content), as reported by Tamor and Vassell.[27] It is known that the C–C sp^3 bonding is promoted by deposition from a source of medium-energy ions.[7,8,10] The resulting films have the highest density and diamond-like character, and the band gap is 1–1.8 eV. As noted above, ΔG is proportional to the stress, density, and bond-angle disorder at sp^2 sites in the films.[27,30] At high bias voltage, the change in the ΔG is consistent with the I_D/I_G ratio evolution and seems to be related to the transition to more graphitic bonding, and the reduction of the local distortions in the film (relaxation process). However, ΔG remains large due to the disordering effects of ion bombardment. So, besides the sp^2 content the distribution and local bonding of the sp^2 bond play a significant role in the electronic properties of a-C:H films.[32–34]

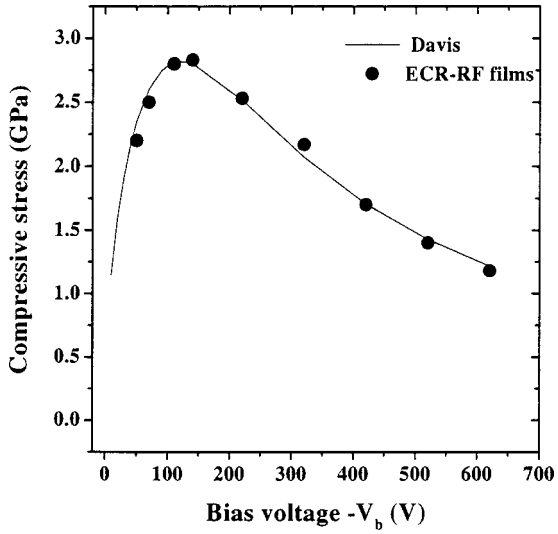

FIG. 7. Intrinsic stress vs negative bias voltage of the hard a-C:H films. The solid curve represents the fitting of Eq. (1) using the Davis model.

D. Intrinsic stress

In Fig. 7 we present the variation of the internal stresses with the bias voltage. It is seen that despite the high hydrogen content in the films, the stresses are found to be in a compressive state.[13] Their magnitude increases abruptly with increasing bias, and passes through a maximum value of about 2.8 GPa for -120 V, and then decreases monotonically for higher bias. The ion bombardment and the penetration of these energetic species into the volume of the growing film can increase the local density or lead to an increase of the compressive local stress as it is observed between -30 and -120 V.[7,8] The transformation of stable C-sp^2 sites to metastable C-sp^3 states can also explain the increase of the compressive local stress.[6] The highest value obtained at -120 V corresponds to films of maximum C–C-sp^3, in good agreement with the result reported in Fig. 6(b), according to Tamor and Vassell.[27] The reduction of stress observed at high bias voltage is probably related to a significant decrease in the concentration of C–C-sp^3 sites, resulting from the phenomena of sputtering, damage, and relaxation of the matrix,

which become more important. This process is accompanied by an increase of the substrate temperature, induced by the energetic particle bombardment. In this study, the substrate holder is water cooled so the temperature of the surface is kept less than 200 °C even at high ion bombardment conditions. Thus, we can assume that the energetic particle bombardment of the surface of growing films is a major factor affecting the compressive stress in the films.

It is interesting to note that the stress variation has the same trend as those obtained for highly tetrahedral amorphous carbon films.[10,12,14] This similarity suggests that the deposition mechanism of these films can be described partially by the subimplantation process, which has been proposed by Davis and Robertson to describe the promotion of the C–C-sp^3 hybridization of ta-C films and the formation of the compressive stress.[7,8] This model is based on incident energetic ions, which can penetrate into the carbon film leading to densification of subsurface layers of evolving film. The decline in the compressive stress can be attributed to ions with high energies penetrating deeper into the film and dissipating their excess energy locally as lattice vibrations or mobile defects, allowing the excess density to relax by atoms migrating back to the surface. The intrinsic stress in a-C films is related to ion energy by the following expression:

$$\sigma \approx \frac{c\sqrt{E}}{R/j + 0.016p(E/E_0)}, \tag{1}$$

where E is the ion energy, E_0 is threshold energy, which activates the relaxation process, R/j is the ratio between the deposition flux to the bombarding ion flux, and p is a material parameter of order 1 according to the thermal spike model.[5]

As previously reported, the subimplantation model has been used to explain the deposition mechanism of ta-C and ta-C:H deposited by techniques in which a monoenergetic ion beam is used.[7,8,10] In the ECR plasma system, the situation is more complex. The formation of the carbon films with a high fraction of sp^3-C (DLC) bonds results from two features of the deposition process. First, there is the high ionization of the plasma beam, which can increase the density. Second, the presence of one predominant ion species leads to subimplantation by monoenergetic ion species. Each of these factors contributes to the hydrogen incorporation and the sp^3 fraction found in DLC films. The mean role of C–C-sp^3 sites is to generate the compressive stress in the films.[17,18]

According to Zarrabian *et al.*,[17,18] the mass spectrum of methane reveals that $C_2H_5^+$ and CH_5^+ appear as the major group of ions in the plasma. An increase in bias voltage from -30 to -600 V at low pressure (2.6 mTorr), leads to a higher decomposition of the injected gas which is a source of the principal ion–molecule reaction. As a result, a relative increase of H_x^+, CH_x^+ species and a decrease in $C_2H_x^+$ is observed.[17,18] In addition, $C_2H_5^+$ ions do not easily dissociate because of their strong C≡C bond (C-sp^1). Thus, to calculate the energy per atoms E_C is very difficult. Finally, the films were prepared as a function of the negative bias voltage. This parameter does not represent the effective energy of the ions striking the film, as required in Eq. (1). However, considering that at low plasma pressure (0.35 Pa here) the ion collisions in the sheath width are not significant, a good approximation of ion energy E is given by

$$E = q(V_p - V_b) \pm 1/2\Delta E, \tag{2}$$

where V_p is the plasma potential (≈20 V) and V_b is the bias voltage and the modulation ΔE is defined as

$$\Delta E = \frac{4}{\pi}\frac{1}{\omega}\left[\frac{e^2 n_i}{m_i \epsilon_0}\right]^{1/2} q(V_p - V_b), \tag{3}$$

with e the charge of electron, ϵ_0 the the permitivity of free space, and ω the frequency of discharge: n_i and m_i design density and mass of ions, respectively.

The stress data of Fig. 7 were then fitted using Eq. (1). The best fitted parameters found are given in Table I. This value is of the same order as those obtained in both ta-C and ta-C:H films.[10,12,14] It was suggested that E_0 has a value between 2.5 and 3 eV due to the film thermal stability, which gives $p \approx 0.1$.[14] The R/j flux ratio is similar to typical values reported in the literature.[11,35] Using the estimations of Zarrabian *et al.*,[17,18] the highest stresses obtained were at the bias voltage of about -120 V, corresponding to an ion energy of about 160 eV for $C_2H_5^+$ and CH_5^+. This ion energy is similar to the typical values reported in the literature.[10–12,14] The mean energy per carbon atom E_{Cmean} will be approximately twice for CH_5^+ ($E_{Cmean} \approx 122$ eV) as that of $C_2H_5^+$ species ($E_{Cmean} \approx 66$ eV) and still similar to those obtained for ta-C (140 eV) and for ta-C:H (92 eV). Nevertheless, the agreement between the experimental results and predicted data, as shown in Fig. 7, together with the similarity of the maximum energy position and the sharp peak obtained, supports the interpretation that the deposition of a-C:H films using (CH_4+Ar) mixture decomposition in the ECR-rf system is, indeed, controlled by the ion subimplantation process, as in the case of tetrahedral amorphous carbon films.[10,12,14]

TABLE I. Experimental values of fitting parameters included in Eq. (1) based on the model proposed by Davis.

Fitting parameters	ECR-rf plasma
c	0.58
R/j	1.58
$p(E_0)^{-5/3}$	0.0012

IV. CONCLUSION

Hard a-C:H films have been deposited using a dual ECR-rf discharge of methane–argon (5%) mixture at low pressure. The films are amorphous and exhibit high H content. The FTIR and ERDA experiments showed a decrease in the total H bonded and content with increasing bias. The correlation between the G and D peaks evolution and ion energy is similar to that found for ta-C and ta-C:H. The relative intensity of the D over G band (I_D/I_G ratio) increases from 0.34 to 1.92 in the same range of bias voltage. This trend is associated with the increase in the number of C-sp^2 sites and supported the reduction of the optical gap (E_{04} and E_{Tauc}). We have confirmed that the deposition process of the films is controlled by the subimplantation model proposed by

Davis and Robertson to describe the formation of the sp^3 rich phase in films prepared by techniques that use monoenergetic species. In the ECR plasma, the ions sticking the film surface are not monoenergetic. The stress data match the subimplantation model and the optimum energy of 160 eV, which corresponds to the more diamond-like character of the films, is similar to those obtained in the literature. The origin of the stress is discussed as a function of the deposition process, which can be considered as a combination of the subimplantation model leading to an increase of the compressive stress in the films and an additional relaxation process, resulting from the reduction of H content and the increase of C-sp^2 sites.

ACKNOWLEDGMENTS

The authors would like to thank Dr. M. R. Kré and Professor G. Turban from the Institut des Matériaux de Nantes, for preparation of the samples. They gratefully acknowledge the help of A. Grossman for ERDA measurements. This work was supported by the Interreg II program.

[1] W. Jacob, Thin Solid Films **326**, 1 (1998).
[2] J. C. Angus, C. C. Hayman, and R. W. Hoffman, J. Vac. Sci. Technol. A **9**, 2459 (1991).
[3] *Amorphous Hydrogenated Carbon Films*, edited by P. Koild and P. Oelhafen, Proceedings of European Materials Conference.
[4] J. Robertson, Philos. Mag. Lett. **57**, 143 (1988).
[5] Y. Lifshitz, S. R. Kasiand, and J. W. Rabelais, Phys. Rev. Lett. **68**, 620 (1989).
[6] D. R McKenzie, D. Müller, and B. A. Pailthorpe, Phys. Rev. Lett. **67**, 773 (1991).
[7] C. A. Davis, Thin Solid Films **266**, 30 (1993).
[8] J. Robertson, Diamond Relat. Mater. **2**, 284 (1993).
[9] H. Windishmann, J. Appl. Phys. **62**, 1800 (1987); Crit. Rev. Solid State Mater. Sci. **17**, 547 (1992).
[10] M. Weiller, S. Sattel, T. Giessen, K. Jung, H. Ehrhardt, V. S. Veerasamy, and J. Robertson, Phys. Rev. B **53**, 1594 (1996).
[11] R. G. Lacerda and F. C. Marques, Appl. Phys. Lett. **73**, 617 (1998).
[12] S. Sattel, J. Robertson, and H. Ehrhardt, J. Appl. Phys. **82**, 4566 (1997).
[13] B. Racine, M. Benlahsen, K. Zellama, P. Goudeau, M. Zarrabian, and G. Turban, Appl. Phys. Lett. **73**, 3226 (1998).
[14] P. J. Fallon, V. S. Veerasamy, C. A. Davis, J. Robertson, G. A. J. Amaratunga, W. I. Milne, and J. Koskineen, Phys. Rev. B **48**, 4777 (1993).
[15] M. Chhowalla, J. Robertson, S. R. P. Silva, G. A. J. Amaratunga, W. I. Milne, and J. Koskineen, J. Appl. Phys. **81**, 139 (1997).
[16] E. Mounier and Y. Pauleau, Diamond Relat. Mater. **6**, 1182 (1997).
[17] M. Zarrabian, PHD thesis, University of Nantes, Nantes, 1998.
[18] M. Zarrabian, C. Leteinterier, and G. Turban, Plasma Sources Sci. Technol. **7**, 607 (1996).
[19] A. von Keudell, J. Jacob, and W. Fukarek, Appl. Phys. Lett. **66**, 1322 (1995).
[20] A. Horn, A. Schenk, J. Biener, B. Winter, C. Lutterloh, M. Wittman, and J. Küppers, Chem. Phys. Lett. **231**, 3125 (1994).
[21] J. Bellamy, *The Infrared Spectra of Complex Molecules* (Chapman and Hall, London, 1975), Vol. 2.
[22] B. Dishler, R. E. Sah, P. Koidl, W. Fluhr, and A. Wokaun, in *Proceedings of the 7th Symposium on Plasma Chemistry*, edited by C. J. Timmermans (IUPAC, Eindhoven, 1985), p. 45.
[23] V. Paret, PHD thesis, University of Paris VI, Paris, 1999.
[24] V. Paret, A. Sadki, Y. Bounouh, R. Almaeh, C. Naud, M. Zarrabian, A. Seignac, G. Turban, and M. L. Thèye, J. Non-Cryst. Solids **227–230**, 583 (1998).
[25] M. Zarrabian, N. Fourches-Coulon, G. Turban, C. Marhic, and M. Lancin, Diamond Relat. Mater. **6**, 542 (1997).
[26] R. J. Nemanich and S. A. Colin, Phys. Rev. B **20**, 392 (1979).
[27] M. A. Tamor and W. C. Vassell, J. Appl. Phys. **76**, 3823 (1994).
[28] J. Schwan, S. Ulrich, V. Batori, H. Ehrhardt, and S. R. P. Silva, J. Appl. Phys. **80**, 440 (1996).
[29] F. Tuinstra and J. L. Koenig, J. Chem. Phys. **53**, 1126 (1976).
[30] A. C. Ferrari and J. Robertson, Phys. Rev. B **61**, 14095 (2000).
[31] J. Tauc, in *Optical Properties of Solids*, edited by F. Abelès (North Holland, Amsterdam, 1972), p. 277.
[32] J. Robertson, Phys. Rev. B **53**, 16302 (1996).
[33] C. Oppedisano and A. Tagliaferro, Appl. Phys. Lett. **75**, 3650 (1999).
[34] J. Schwan, S. Ulrich, T. Theel, H. Roth, H. Ehrhardt, P. Becker, and S. R. P. Silva, J. Appl. Phys. **82**, 6024 (1997).
[35] R. Kleber, M. Weiller, A. Kruger, S. Sattel, G. Kunz, K. Jung, and H. Ehrhardt, Diamond Relat. Mater. **2**, 246 (1993).